

Noise of a single-electron transistor in the regime of large quantum fluctuations of island charge out of equilibrium

Yasuhiro Utsumi,* Hiroshi Imamura, Masahiko Hayashi, and Hiromichi Ebisawa
Graduate School of Information Sciences, Tohoku University, Sendai 980-8579, Japan

(Dated: February 1, 2008)

By using the drone-fermion representation and the Schwinger-Keldysh approach, we calculate the current noise and the charge noise for a single-electron transistor in the non-equilibrium state in the presence of large quantum fluctuation of island charge. Our result interpolates between those of the “orthodox” theory and the “co-tunneling theory”. We find the following effects which are not treated by previous theories: (i) At zero temperature $T = 0$ and at finite applied bias voltage $|eV| \gg T_K$, where T_K is the “Kondo temperature”, we find the Fano factor is suppressed more than the suppression caused by Coulomb correlation both in the Coulomb blockade regime and in the sequential tunneling regime. (ii) For $T \gg |eV|/2 \gg T_K$, the current noise in the presence of large charge fluctuation is modified and deviates from the prediction of the orthodox theory. However, the Fano factor coincides with that of the orthodox theory and is proportional to the temperature. (iii) For $eV, T \lesssim T_K$, the charge noise is suppressed due to the renormalization of system parameters caused by quantum fluctuation of charge. We interpret it in terms of the modification of the “unit” for island charge.

PACS numbers: 73.23.Hk, 72.70.+m

I. INTRODUCTION

In a small metallic island where the charging energy E_C exceeds the temperature T (we use the unit $k_B = 1$), the Coulomb interaction affects transport properties through the island. The resulting phenomenon is called the Coulomb blockade (CB) and such system is named the single-electron transistor (SET). CB has been attracted much attention in the last decade [1–3] and the nature of the transport properties of SET has been clarified. SET is interesting because it is regarded as one of the most simple examples of strongly correlated system which can be brought into the non-equilibrium state by applied bias voltage. Early investigations consider the case where the tunneling conductance is so small that the higher order quantum fluctuation of island charge is negligible. Recently, the quantum fluctuation in SET has attracted much attention as one of the basic problems in this field. The quantum fluctuation is quantitatively characterized by the dimensionless parallel conductance: $\alpha_0 = R_K / ((2\pi)^2 R_T)$ where $R_K = h/e^2$ is the quantum resistance and R_T is the parallel tunneling resistance of the source and the drain junctions. There has been much development on theoretical investigation in the whole range of α_0 . Especially in the *weak tunneling regime* ($\alpha_0 < 1$), the life-time broadening of a charge state level is much smaller than the typical level spacing of charge states, and thus the effective two-state model, which is equivalent to the multichannel anisotropic Kondo model in the equilibrium state[4], well describes the low-energy physics. With this

model, it is predicted that the quantum fluctuation of charge causes the renormalization of the conductance and the charging energy below the “Kondo temperature” $T_K = \frac{E_C}{2\pi} e^{-1/(2\alpha_0)}$ [4–9]. The renormalization of the conductance is confirmed experimentally as $1/\ln T$ dependence of the conductance peak at low temperature[10]. It is also predicted that in the non-equilibrium state, the dissipative charge fluctuation causes the life-time broadening of a charge state level and smears the structures of I - V characteristic[3, 8, 11].

Though investigations have revealed much about the quantum fluctuation, most of them have been limited to averaged quantities. In order to understand the nature of the quantum fluctuation, investigations on the higher-order correlation function of fluctuation operators are required. A good starting point may be the investigation on the second moment of fluctuation operators, i.e., the noise[12]. The charge noise and the current noise in the weak tunneling regime is also important for practical applications, because it determines the performance of SET electrometers [13–16].

The current noise is defined by the auto-correlation function of the current fluctuation operator $\delta\hat{I}(t) = \hat{I}(t) - \langle \hat{I}(t) \rangle$ as

$$S_{II}(t, t') = \langle \{ \delta\hat{I}(t), \delta\hat{I}(t') \} \rangle, \quad (1)$$

where $\langle \dots \rangle$ means the statistical average. Until recently, investigations on the noise have been done using the framework of the “orthodox” theory[13, 15, 17–19], which takes account of the lowest order quantum fluctuation, namely the sequential tunneling (ST) process. Recently, several authors[14, 20, 21] discussed the higher order quantum fluctuation in CB regime within the “co-tunneling theory”[22]. However, there is no approximation covering both ST and CB regime. The aim of the present work is to construct a theoretical frame-

*Present address Max-Planck-Institut für Mikrostrukturphysik Weinberg 2, D-06120 Halle, Germany

work, which covers both of these regimes for arbitrary α_0 and clarify how the quantum fluctuation affects the noise.

The Keldysh formalism[23–25] has been one of the most powerful methods to study the non-equilibrium properties of mesoscopic systems. However to apply this method to SET in the two-state limit, one must overcome a technical difficulty: The spin-1/2 operator, which is introduced to restrict charge number states by the strong Coulomb interaction, prevents one from utilizing Wick's theorem. The most successful treatment to overcome this problem is given in Ref. [6], in which a formulation of perturbative expansion for the reduced density matrix in the real time domain is developed and the inelastic resonant tunneling processes is treated. The method of Ref. [6] enables one to classify various tunneling processes using diagrammatic techniques, and can be also applied to other systems with the strong local correlation, such as quantum dot[26]. In spite of these successes, it seems to be still difficult to apply this method for the calculation of higher order correlation functions, since this method requires to solve a special integro-differential equation even for the calculation of the average in the presence of large quantum fluctuation[6].

In this paper, we investigate the current noise and the charge noise in the regime of large quantum fluctuation of charge out of equilibrium. We adopt the Schwinger-Keldysh approach and the drone-fermion representation of the effective spin-1/2 operator[27, 28]. Schwinger-Keldysh approach enables us to calculate any order moment systematically by the functional derivative technique[29, 30] satisfying the charge conservation[29], and it helps us in manipulating many complicated terms. The drone-fermion representation allows us to utilize the fermionic Wick's theorem and to take effects of the strong correlation into account. With the help of this technique, we can extensively take account of the higher order processes of tunneling. We will show that our approximation reproduces the resonant tunneling approximation (RTA)[6] as for the average current and the average charge.

The outline of this paper is as follows. In Sec. II, we briefly summarize the Keldysh formalism and introduce an approximate generating functional. We also show that the average and the noise expressions can be derived using the functional derivation. In Sec. III, we actually calculate the average current, the average charge, the current noise and the charge noise. In Sec. IV we show numerical results for the noise and give some discussions on the non-equilibrium fluctuation, the thermal fluctuation and the renormalization effect. Section V summarizes our results.

II. KELDYSH FORMALISM AND GENERATING FUNCTIONAL

A. Brief introduction of the Keldysh formalism

In this section, we give preliminary definitions of the Schwinger-Keldysh approach and we summarize three useful representations: the *closed time-path*, the *single time* and the *physical* representations (Sec. 2 of Ref. [25]). For simplicity, we consider the following action of a free fermion with a linear source term to explain the basic formalism:

$$S = \int_C dt \{a(t)^* (i\hbar \partial_t - \varepsilon) a(t) + a(t) J^*(t) + h.c.\}, \quad (2)$$

where the closed time path C consists of the forward branch C_+ , the backward branch C_- and the imaginary time-path C_τ as shown in Fig. 1[31]. $a(t)$ is a Grassmann variable satisfying the anti-periodic boundary condition $a(-\infty \in C_+) = -a(-\infty - i\hbar\beta \in C_\tau)$. The complex variable $J(t)$ is defined only on the forward and backward branch $C_+ + C_-$. The generating functional for the connected closed time-path Green function (GF) is defined as,

$$W = -i\hbar \ln Z, \quad Z = \int \mathcal{D}[a^*, a] \exp(-S/i\hbar).$$

GF in the closed time-path representation is obtained by the second derivative of the generating functional with respect to $J(t)$ ($t \in C_+ + C_-$):

$$-G(1, 2) = \frac{\delta^2 W}{\delta J(1)^* \delta J(2)} \Big|_{J=0}. \quad (3)$$

Hereafter, we use arguments 1, 2 instead of t_1, t_2 for short.

Though the closed time-path representation makes the formulation compact, in order to obtain the physical quantities, we sometimes need the single time representation in which the time on C is projected onto the real axis. In this representation the degrees of freedoms of fields are doubled which we denote as,

$$\hat{J}(t) = \begin{pmatrix} J_+(t) \\ J_-(t) \end{pmatrix}, \quad (4)$$

etc. Here $J_\pm(t)$ is defined on C_\pm and t is the real time. In the same way as J , GF is transformed into 2×2 matrix in the Keldysh space:

$$\hat{G}(1, 2) = \begin{pmatrix} G^{++}(1, 2) & G^{+-}(1, 2) \\ G^{-+}(1, 2) & G^{--}(1, 2) \end{pmatrix}. \quad (5)$$

Here, arguments t_1 and t_2 are the real time and each component is defined with the statistical average in the path integral representation $\langle A \rangle = \int \mathcal{D}[a^*, a] A \exp(-S/i\hbar) / Z|_{J=0}$ as $G^{ij}(1, 2) = \langle a_i(1) a_j(2)^* \rangle|_{J=0} / (i\hbar)$. Diagonal components G^{++} and

G^{--} are the causal and the anti-causal GF, respectively. Off-diagonal components are correlation functions, which are written in the operator representation as $G^{-+}(1, 2) = \langle \hat{a}(1) \hat{a}(2)^\dagger \rangle / (i\hbar)$ and $G^{+-}(1, 2) = -\langle \hat{a}(2)^\dagger \hat{a}(1) \rangle / (i\hbar)$ [25]. Here the statistical average is defined as $\langle \hat{A} \rangle = \text{Tr}[e^{-\beta \hat{H}_0} \hat{A}] / Z_0$ where the Hamiltonian operator \hat{H}_0 is $\varepsilon \hat{a}^\dagger \hat{a}$ and the partition function Z_0 is given as $\text{Tr}[e^{-\beta \hat{H}_0}]$.

It is known that four components of Eq. (5) are not independent. This redundancy is removed by the Keldysh rotation[24, 25]. After the rotation, we obtain the so-called physical representation:

$$\tilde{J} = \begin{pmatrix} J_1 \\ J_2 \end{pmatrix} = \frac{1}{\sqrt{2}} \begin{pmatrix} J_+ - J_- \\ J_+ + J_- \end{pmatrix}, \quad (6)$$

$$\tilde{G}(1, 2) = \begin{pmatrix} 0 & G^A(1, 2) \\ G^R(1, 2) & G^K(1, 2) \end{pmatrix}. \quad (7)$$

GFs denoted by superscripts, A , R and K are advanced, retarded and Keldysh components, respectively. In the practical calculations, instead of J_1 and J_2 , the center-of-mass coordinate J_c and the relative coordinate J_Δ ,

$$\begin{cases} J_c(t) = \frac{J_+(t) + J_-(t)}{2} = J_2(t)/\sqrt{2} \\ J_\Delta(t) = J_+(t) - J_-(t) = J_1(t)\sqrt{2} \end{cases}, \quad (8)$$

are used in most cases.

There are the following relations between components of GF:

$$\begin{aligned} G^{--}(1, 2) + G^{++}(1, 2) &= G^{-+}(1, 2) + G^{+-}(1, 2) \\ &= \frac{1}{i\hbar} \langle \{ \hat{a}(1)^\dagger, \hat{a}(2) \} \rangle = G^K(1, 2), \end{aligned} \quad (9)$$

$$\begin{aligned} G^R(1, 2) - G^A(1, 2) &= G^{-+}(1, 2) - G^{+-}(1, 2) \\ &= \frac{1}{i\hbar} \langle [\hat{a}(1), \hat{a}^\dagger(2)] \rangle = G^C(1, 2). \end{aligned} \quad (10)$$

Here we introduce a notation G^C whose physical meaning is the spectral density in the energy space. Equation (9) is derived from the normalization of the step function (see Eq. (2.67) in Ref. [25]).

The normalization condition of the density matrix results in an important equation $Z|_{J=0}/Z_0 = 1$ (see Sec. 2.4 of Ref. [25])[32] which is equivalent to the following equations:

$$\left. \frac{\delta W}{\delta J_c(1)} \right|_{J_\Delta=0} = \left. \frac{\delta^2 W}{\delta J_c(1) \delta J_c(2)} \right|_{J_\Delta=0} = \dots = 0. \quad (11)$$

B. Model Hamiltonian in the drone-fermion representation and the generating functional in closed time path - path integral representation

In this section, we introduce our model Hamiltonian and derive the generating functional for SET, based on which we construct the perturbation theory.

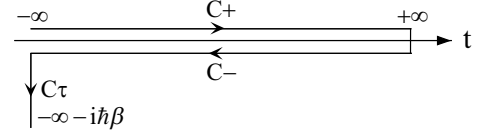


FIG. 1: The closed time-path going from $-\infty$ to ∞ (C_+), going back to $-\infty$ (C_-), connecting the imaginary time path C_τ and closing at $t = -\infty - i\hbar\beta$.

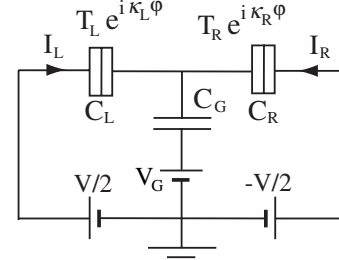


FIG. 2: The equivalent circuit of a SET.

Figure 2 shows the equivalent circuit of a SET. A metallic island exchanges electrons with the left (right) lead via a tunnel junction characterized by the tunneling matrix element $T_{L(R)}$. The island is coupled to leads and a gate via capacitors C_L , C_R and C_G . We consider in the weak tunneling regime $\alpha_0 < 1$ and use the two-state model. In this paper, we limit ourselves to the symmetric case: $C_L = C_R$ and $T_L = T_R$. The total Hamiltonian consists of the unperturbed part \hat{H}_0 and the tunneling part \hat{H}_T . Omitting a trivial constant, the unperturbed part is given as

$$\hat{H}_0 = \sum_{r=L,R,I} \sum_{k,n} \varepsilon_{rk} \hat{a}_{rkn}^\dagger \hat{a}_{rkn} + \Delta_0 \frac{\hat{\sigma}_z + 1}{2}, \quad (12)$$

where \hat{a}_{rkn} is the annihilation operator of an electron with wave vector k in the left (right) lead ($r = L(R)$) or in the island ($r = I$). The subscript n numbers the transverse channels including spin degree of freedom. The density of states is considered as constant in each region: $\rho_r(\varepsilon) = \sum_k \delta(\varepsilon - \varepsilon_{rk}) = \rho_r$ ($r = L, R, I$). The second term is the charging energy and the effective spin-1/2 operator $\hat{\sigma}$ acts on the lowest two charge states. The energy difference between two charge states is given by $\Delta_0 = E_C(1 - 2Q_G/e)$ where Q_G is the gate charge.

The tunneling Hamiltonian

$$\hat{H}_T(t) = \sum_{\substack{r=L,R \\ k,k',n}} T_r e^{i\kappa_r \varphi(t)} \hat{a}_{Ikn}^\dagger \hat{a}_{rk'n} \hat{\sigma}_+ + \text{h.c.}, \quad (13)$$

describes the electron tunneling across the junctions and simultaneous change of the charge state of the island. $\varphi(t) = eVt/\hbar$ is the phase difference between the left and the right leads and parameters $\kappa_L = -\kappa_R = 1/2$ characterizes the voltage drop between the left (right) lead and the island. The tunneling Hamiltonian is adiabatically

turned on in the remote past and off in the distant future. It is the widely adopted procedure, which ensures the time translational invariance to describe a stationary state.

In order to utilize Wick's theorem for fermions, we employ the mapping of the effective spin-1/2 operator onto two fermion operators \hat{c} and \hat{d} [27, 28, 33]: $\hat{\sigma}_+ = \hat{c}^\dagger \hat{\phi}$, $\hat{\sigma}_z = 2\hat{c}^\dagger \hat{c} - 1$, where $\hat{\phi} = \hat{d}^\dagger + \hat{d}$ is a Majorana fermion operator ($\hat{\phi}^2 = 1$). This representation is called drone-fermion representation [28], because $\hat{\phi}$ is a “drone” whose only job is to make spin-1/2 operators of different spins commute, rather than anti-commute [33].

Employing the Hamiltonian operator in the drone-fermion representation and following the standard manner to introduce a path integral [34], we obtain the generating functional in the path integral representation:

$$Z = \int \mathcal{D}[a_{rkn}^*, a_{rkn}, c^*, c, d^*, d] \exp\left(-\frac{S}{i\hbar}\right), \quad (14)$$

where all field variables are Grassmann variables satisfying the anti-periodic boundary condition. The action is given by

$$\begin{aligned} S = & \int_C dt \{ c(t)^* (i\hbar \partial_t - h(t)) c(t) + i\hbar d(t)^* \partial_t d(t) \\ & + \sum_{r,k,n} a_{rkn}(t)^* (i\hbar \partial_t - \varepsilon_{rk}) a_{rkn}(t) \\ & + \sum_{\substack{r=L,R \\ k,k',n}} T_r e^{i\varphi_r(t)} a_{rkn}(t)^* a_{Ik'n}(t) \sigma_+(t) + \text{h.c.} \}, \end{aligned} \quad (15)$$

where, $\varphi_r(t) = \kappa_r \varphi(t)$. In Eq. (15) we introduced auxiliary source fields, $h(t)$ and $\varphi(t)$, in order to calculate the average and the noise by the functional derivation. It is noticed that the degrees of freedoms are doubled, as shown in Eq. (4). After the derivation, these variables are put as $h_\pm(t) = \Delta_0$ and $\varphi_\pm(t) = eVt/\hbar$ to be related with the parameters of the actual system.

By introducing a linear source term $\int_C d1 J(1) \phi(1)$, where J is a Grassmann variable, all fields can be traced out [35]. In the limit of large transverse-channel number, Z is expressed as [36]

$$\begin{aligned} Z = & \exp\left(-\sum_n \frac{(i\hbar)^{2n}}{n} \text{Tr} \left[\left(g_c \frac{\delta}{\delta J} \alpha \frac{\delta}{\delta J} \right)^n \right]\right) \\ & \times \exp\left(-\frac{1}{2i\hbar} \int_C d1 d2 J(1) g_\phi(1, 2) J(2)\right) \Big|_{J=0} \\ & \times 2e^{\text{Tr}[\ln g_c^{-1}]}, \end{aligned} \quad (16)$$

where we omitted the partition function of noninteracting electrons. The trace Tr and the products represent the integration along C as follows,

$$\text{Tr}[g_c J g_\phi] = \int_C d1 d2 g_c(1, 2) J(2) g_\phi(2, 1).$$

The particle-hole GF $\alpha = \sum_{r=L,R} \alpha_r$, in the closed time-path form is written as

$$\alpha_r(1, 2) = -i\hbar N_{\text{ch}} T_r^2 g_r(1, 2) g_l(2, 1) e^{i(\varphi_r(1) - \varphi_r(2))}, \quad (17)$$

where N_{ch} is the number of the transverse channels. The GF for free electron in the lead r ($= L, R$) and the island r ($= I$), $g_r(t, t') = \sum_k g_{rk}(t, t')$, is given as

$$g_{rkn}^{-1}(t, t') = (i\hbar \partial_t - \varepsilon_{rk}) \delta(t, t'), \quad (18)$$

which satisfies the anti-periodic boundary condition: $g_{rkn}(t, -\infty \in C_+) = -g_{rkn}(t, -i\hbar\beta - \infty)$. The c -field and the d -field GFs defined by

$$g_c^{-1}(t, t') = (i\hbar \partial_t - h(t)) \delta(t, t'), \quad (19)$$

$$g_\phi^{-1}(t, t') = i\hbar \partial_t \delta(t, t')/2, \quad (20)$$

also satisfy the anti-periodic boundary condition.

Using Eq. (16), we construct a systematic perturbation expansion in terms of α . For example, we show the diagrammatic representation of the zeroth ($W^{(0)}$), the first ($W^{(1)}$) and the second order contribution ($W^{(2)}$) to the generating functional W in Fig. 3. Here, solid lines, dotted lines and wavy lines represent GFs for c -field, d -field and particle-hole, respectively. Practical forms are given as follows:

$$W^{(0)} = -i\hbar \text{Tr} [\ln g_c^{-1}], \quad (21)$$

$$W^{(1)} = i\hbar \text{Tr} [g_c \Sigma_c], \quad (22)$$

$$W_{c\text{-field}}^{(2)} = \frac{i\hbar}{2} \text{Tr} [(g_c \Sigma_c)^2], \quad (23)$$

where $W_{c\text{-field}}^{(2)}$ is the term corresponding to the first diagram in Fig. 3 (c), which we call the c -field correction. The other four diagrams can be written in the same way. Here, the self-energy of the c -field $\Sigma_c(1, 2) = \sum_{r=L,R} \Sigma_r(1, 2)$ is defined as

$$\Sigma_r(1, 2) = -i\hbar \alpha_r(1, 2) g_\phi(2, 1). \quad (24)$$

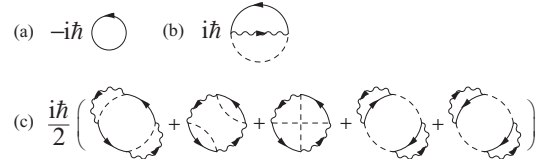


FIG. 3: The diagrammatic representation of (a) $W^{(0)}$, (b) $W^{(1)}$ and (c) $W^{(2)}$. Solid lines, dotted lines and wavy lines represent GFs for c -field, d -field and particle-hole in the closed time-path representation, respectively.

In a previous paper [36], we have shown that the first order contribution causes the divergence at the degeneracy point $\Delta_0 = 0$ for average charge. In order to regularize the divergence, we proposed an approximate generating functional obtained by summing up c -field corrections

$(g_c \Sigma_c)^n$ to infinite order:

$$\begin{aligned} \bar{W} &= -i\hbar \text{Tr} [\ln G_c^{-1}] \\ &= -i\hbar \left(\text{Tr} [g_c^{-1}] - \sum_{n=1}^{\infty} \frac{1}{n} \text{Tr} [(g_c \Sigma_c)^n] \right). \end{aligned} \quad (25)$$

Figure 4 (a) shows the diagrammatic representation of \bar{W} . The circle represents the self-energy of c -field and the thick line represents the full c -field GF defined by the Dyson equation

$$G_c^{-1}(t, t') = g_c^{-1}(t, t') - \Sigma_c(t, t'), \quad (26)$$

whose diagrammatic representation is shown in Fig. 4 (b). In Sec. III B we will show that \bar{W} reproduces results of RTA for the normal metal island. In Sec. III C, we calculate the charge noise and the current noise based on \bar{W} .

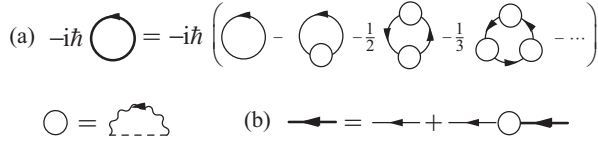


FIG. 4: (a) An approximate generating functional including infinite order c -field correction. The circle is the self-energy of the c -field. (b) The Dyson equation for full c -field GF in the closed time-path representation.

C. Formally exact expressions for average and noise and the charge conservation

In this section, we summarize expressions for the average and the noise on the basis of functional derivative. Relations between physical quantities in the generating functional representation and those in the operator representation are demonstrated in Appendix A. We also show that the gauge invariance of generating functional leads to the charge conservation law.

The exact average current expression is given by the functional derivative of exact generating functional W with respect to the phase difference [29, 30]:

$$I(t) = \left. \frac{e}{\hbar} \frac{\delta W}{\delta \varphi_{\Delta}(t)} \right|_{\varphi_c(t)=eVt/\hbar, h_c(t)=\Delta_0, \varphi_{\Delta}=h_{\Delta}=0}. \quad (27)$$

The center-of-mass coordinate of the phase difference is determined by the Josephson relation [37, 38]. The relative coordinates are put to zero because they are the fictitious variables. From now on, we suppress the equations in the subscript after the vertical bar for short. The average charge is calculated by the functional derivation in terms of the scalar potential of c -field as

$$\frac{Q(t)}{e} = \frac{1}{2} - \left. \frac{\delta W}{\delta h_{\Delta}(t)} \right|. \quad (28)$$

The current noise and the charge noise defined as Eq. (1) are given by the second derivative with respect to φ_{Δ} and h_{Δ} [39]:

$$S_{II}(t, t') = \frac{2e^2}{i\hbar} \frac{\delta^2 W}{\delta \varphi_{\Delta}(t) \delta \varphi_{\Delta}(t')} \Big| - \frac{(\Delta \rightarrow c)}{4}, \quad (29)$$

$$S_{QQ}(t, t') = 2e^2 \frac{-i\hbar \delta^2 W}{\delta h_{\Delta}(t) \delta h_{\Delta}(t')} \Big| - \frac{(\Delta \rightarrow c)}{4}, \quad (30)$$

where $(\Delta \rightarrow c)$ is obtained from the first term by replacing subscripts Δ with c .

It is convenient to rewrite Eq. (27) in the form of the linear combination of the tunneling current at the left junction I_L and that at the right junction I_R as $I(t) = \sum_{r=L,R} \kappa_r I_r(t)$. In the same way, Eq. (29) is written in terms of the correlation function of \hat{I}_r and $\hat{I}_{r'}$ ($r, r' = L, R$), which we denote by $S_{I_r I_{r'}}$, as $S_{II}(t, t') = \sum_{r, r'=L,R} \kappa_r \kappa_{r'} S_{I_r I_{r'}}(t, t')$. Here, I_r and $S_{I_r I_{r'}}$ are written as

$$I_r(t) = \left. \frac{e}{\hbar} \frac{\delta W}{\delta \varphi_{r\Delta}(t)} \right|, \quad (31)$$

$$S_{I_r I_{r'}}(t, t') = \left. \frac{2e^2}{i\hbar} \frac{\delta^2 W}{\delta \varphi_{r\Delta}(t) \delta \varphi_{r'\Delta}(t')} \right| - \frac{(\Delta \rightarrow c)}{4}, \quad (32)$$

by regarding φ_L and φ_R as formally independent variables.

The generating functional Eq. (14) is invariant under the gauge transformation, i.e., the phase transformation of the c -field and the change of the c -field scalar potential:

$$\begin{cases} \varphi_r(t) \rightarrow \varphi_r(t) + \delta\psi(t) \\ h(t) \rightarrow h(t) - \hbar \delta(\partial_t \psi(t)) \end{cases}, \quad (33)$$

where $\delta\psi$ is defined on $C_+ + C_-$. The relation between the gauge invariance and the charge conservation in the non-equilibrium state has been analyzed in Ref. [29]. For our system, the following expressions of the current continuity and the charge conservation for correlation functions

$$\partial_t Q(t) = \sum_{r=L,R} I_r(t), \quad (34)$$

$$\partial_t \partial_{t'} S_{QQ}(t, t') = \sum_{r, r'=L,R} S_{I_r I_{r'}}(t, t'), \quad (35)$$

can be proved (Appendix. B).

III. APPROXIMATE EXPRESSIONS FOR NOISE

In this section, we derive approximate current noise and charge noise expressions, which is main purpose of this paper. We summarize GFs in the physical representation in Sec. III A which are needed for practical calculations. In Sec. III B we calculate the average charge

and the average current and show that our approximation completely reproduces the results of RTA. We also give some notes on the diagrammatic rule suitable for the functional derivative technique. In Sec. III C, we calculate the current noise and the charge noise based on the diagrammatic rule. We will check that our results satisfy the charge conservation law and the fluctuation-dissipation theorem.

A. Fourier transformation of free Green functions

We summarize the Fourier transformation of the retarded and the Keldysh component of GFs. Hereafter in this subsection, we put the auxiliary source fields as shown in the subscript of Eq. (27). The solutions of differential equations (19) and (20) imposing anti-periodic boundary condition are [35]

$$g_\phi^R(\varepsilon) = 2/(\varepsilon + i\eta), \quad g_\phi^K(\varepsilon) = 0, \quad (36)$$

$$\begin{cases} g_c^R(\varepsilon) = 1/(\varepsilon + i\eta - \Delta_0) \\ g_c^K(\varepsilon) = -2i\pi \tanh\left(\frac{\varepsilon}{2T}\right) \delta(\varepsilon - \Delta_0) \end{cases}, \quad (37)$$

where η is a positive infinitesimal number and the δ -function in the energy space is defined as

$$\delta(\varepsilon) = \eta/(\pi(\varepsilon^2 + \eta^2)). \quad (38)$$

The advanced component is the complex conjugate of the retarded component: $g_{\phi(c)}^A(\varepsilon) = g_{\phi(c)}^R(\varepsilon)^*$.

The two components of particle-hole GF are given by,

$$\begin{cases} \alpha_r^R(\varepsilon) = -i\pi\alpha_r^0\rho(\varepsilon - \mu_r) \\ \alpha_r^K(\varepsilon) = -2i\pi\alpha_r^0\rho(\varepsilon - \mu_r) \coth\left(\frac{\varepsilon - \mu_r}{2T}\right) \end{cases}, \quad (39)$$

where $\mu_r = \kappa_r eV$ (Appendix. C). α_r^0 is the dimensionless conductance for tunnel junction r written in terms of the tunnel resistance R_r as $\alpha_r^0 = R_K/((2\pi)^2 R_r) = N_{\text{ch}} T_r^2 \rho_1 \rho_r$. The spectral density of the particle-hole propagator is given by $\rho(\varepsilon) = \varepsilon E_C^2/(\varepsilon^2 + E_C^2)$ where the Lorentzian cut-off function is introduced [6]. The Keldysh component and the component defined by Eq. (10) for the c -field self-energy Eq. (24) and those for the particle-hole GF are related to each other:

$$\Sigma_r^K(\varepsilon) = \alpha_r^C(\varepsilon), \quad \Sigma_r^C(\varepsilon) = \alpha_r^K(\varepsilon). \quad (40)$$

The retarded component of the self-energy is given as

$$\begin{aligned} \Sigma_r^R(\varepsilon) = \alpha_r^r \rho(\varepsilon) & \left\{ 2\text{Re} \psi \left(i \frac{\varepsilon - \mu_r}{2\pi T} \right) \right. \\ & \left. - \psi \left(1 + \frac{E_C}{2\pi T} \right) - \psi \left(\frac{E_C}{2\pi T} \right) \right\} + \frac{\alpha_r^K(\varepsilon)}{2}, \end{aligned} \quad (41)$$

where ψ is the digamma function. The full c -field GF is obtained by solving the Dyson equation in the closed time-path representation Eq. (26) [36]:

$$\begin{cases} G_c^R(\varepsilon) = 1/(\varepsilon + i\eta - \Delta_0 - \Sigma_c^R(\varepsilon)) \\ G_c^K(\varepsilon) = G_c^R(\varepsilon) \{ \Sigma_c^K(\varepsilon) - 2i\eta \tanh\left(\frac{\varepsilon}{2T}\right) \} G_c^A(\varepsilon) \end{cases}, \quad (42)$$

where we used the definition of δ -function Eq. (38). Here we remark the following: Equation (42) shows that in the limit of $\eta \rightarrow 0$, the charge states are independent of the initial equilibrium distribution, because the Keldysh component of c -field GF represents the distribution of charge states. This fact suggests that \bar{W} describes a physically reasonable non-equilibrium stationary state, which should not depend on any initial state.

We transform above expressions into single-time representation. Employing Eqs. (9) and (10) we obtain

$$\alpha_r^{\pm\mp}(\varepsilon) = -2i\pi\alpha_r^r \rho(\varepsilon - \mu_r) n_r^\mp(\varepsilon) = \mp \alpha_r^K(\varepsilon) f_r^\mp(\varepsilon), \quad (43)$$

$$\Sigma_r^{\pm\mp}(\varepsilon) = \mp \alpha_r^{\pm\mp}(\varepsilon), \quad (44)$$

$$G_c^{\pm\mp}(\varepsilon) = \mp |G_c^R(\varepsilon)|^2 \alpha^{\pm\mp}(\varepsilon). \quad (45)$$

Here $f_r^-(\varepsilon) = f^-(\varepsilon - \mu_r)$ and $n_r^-(\varepsilon) = n^-(\varepsilon - \mu_r)$ are written with the Fermi function $f^-(\varepsilon) = 1/(e^{\beta\varepsilon} + 1)$ and the Bose distribution function $n^-(\varepsilon) = 1/(e^{\beta\varepsilon} - 1)$. Functions f^+ and n^+ are given by $f^+(\varepsilon) = f^-(\varepsilon) e^{\beta\varepsilon}$ and $n^+(\varepsilon) = n^-(\varepsilon) e^{\beta\varepsilon}$, respectively.

B. Reformulation of the resonant tunneling approximation

The reason why we adopt the generating functional approach is that once an approximate generating functional is obtained, one can calculate any order moment systematically by the functional derivation. In the following sections we perform practical calculations, employing \bar{W} introduced in Sec. II B. Detailed discussions on our approximation are retained in Appendix D.

The average current is calculated by substituting \bar{W} into Eq. (31) [36]:

$$\begin{aligned} I_r(t) &= \frac{e}{\hbar} \frac{\delta \bar{W}}{\delta \varphi_{r\Delta}(t)} \Big| \\ &= -e \text{Tr} \left[G_c \frac{\delta \varphi_r}{\delta \varphi_{r\Delta}(t)} \Sigma_r - G_c \Sigma_r \frac{\delta \varphi_r}{\delta \varphi_{r\Delta}(t)} \right] \Big|. \end{aligned} \quad (46)$$

Here, we used the fact that the self-energy Eq. (24) includes the phase factor through the particle-hole GF Eq. (17). In the language of Feynmann diagrams, Eq. (46) can be rewritten in a compact form:

$$I_r(t) = -e \left[\text{Diagram 1} - \text{Diagram 2} \right] \Big|. \quad (47)$$

Solid dots with t represents $\delta\varphi_r/\delta\varphi_{r\Delta}(t)$. The circle with r is the partial self-energy defined by Eq. (24). Here we obtain the diagrammatic rule similar to that of Refs. [40, 41].

(i) The diagrams corresponding to the functional derivative with respect to $\varphi_{r\Delta}(t)$ is obtained by a series of the following operations; to put a solid dot

onto all possible positions of vertices in a closed diagram, to assign r on a circle connected to the solid dot, to multiple i , and to assign minus sign if a solid line comes into the solid dot.

Next we project the fictitious time on C to the real axis. As the tunneling Hamiltonian is zero on C_τ , $\Sigma_r(t, t')$ is zero for $t \in C_\tau$ or $t' \in C_\tau$. Hence, the diagrams in Eq. (47) are rewritten as,

$$\text{Tr} \left[\tilde{G}_c \frac{\delta \tilde{\varphi}_r}{\delta \varphi_{r\Delta}(t)} \tilde{\Sigma}_r \tau^1 - \tilde{G} \tau^1 \tilde{\Sigma}_r \frac{\delta \tilde{\varphi}_r}{\delta \varphi_{r\Delta}(t)} \right], \quad (48)$$

where we performed the Keldysh rotation. τ^s ($s = 0, 1, 2, 3$) is the Pauli matrix in the Keldysh space [24]. The trace is carried out over the Keldysh space and products represents the integration along the real-time as

$$\text{Tr} [\tilde{g}_\phi \tilde{\varphi} \tilde{g}_\phi] = \int_{-\infty}^{\infty} d1 d2 \text{Tr} [\tilde{g}_\phi(1, 2) \tilde{\varphi}(2) \tilde{g}_\phi(2, 1)].$$

The phase in the physical representation $\tilde{\varphi}_r$ is written as $\tilde{\varphi}_r(t) = \varphi_{rc}(t) \tau^1 + \varphi_{r\Delta}(t) \tau^0/2$, which leads to a useful relation for the functional derivative technique:

$$\delta \tilde{\varphi}_r(t') / \delta \varphi_{r\Delta}(t) = \tau^0 \delta(t - t')/2. \quad (49)$$

By using the property of the GF in the physical representation $\tilde{G}(t, t')^\dagger = -\tau^3 \tilde{G}(t', t) \tau^3$, and that of a Pauli matrix $\tau^3 \tau^1 \tau^3 = -\tau^1$, we can see that the second term of Eq. (48) is minus the complex conjugate of the first term. To generalize this property, we obtain a helpful rule to reduce the number of diagrams: A diagram which is complex conjugate of a certain diagram is obtained by changing the direction of all lines and putting minus sign if the diagram includes odd numbers of vertices without solid dot.

By performing the Fourier transformation, we rewrite Eq. (47) as:

$$2e\text{Re} \left[\text{Diagram} \right] = 2e\text{Re} \int \frac{d\varepsilon}{h} \text{Tr} \left[\tilde{G}_c(\varepsilon) \frac{\tau^0}{2} \tilde{\Sigma}_r(\varepsilon) \tau^1 \right] \quad (50)$$

$$= e \int \frac{d\varepsilon}{h} \frac{\Sigma_r^C(\varepsilon) G_c^K(\varepsilon)}{2} - (C \leftrightarrow K). \quad (51)$$

The second term ($C \leftrightarrow K$) is obtained from the first term by swapping superscripts K and C . By generalizing Eq. (50), we obtain the rule to calculate the diagram:

(ii) Put 2×2 matrix GFs in the physical representation to the corresponding lines and circles, put $\tau^0/2$ or τ^1 to a vertex with or without solid dot. Subsequently, carry out the trace over Keldysh space and the integration over the frequency ε/h .

Employing Eqs. (9) and (10), Eq. (51) is transformed into the single time representation: $(e/h) \int d\varepsilon \Sigma_r^{+-}(\varepsilon) G_c^{-+}(\varepsilon) - (+ \leftrightarrow -)$. By using Eqs. (43),

(44) and (45), and noting $I(t) = I_L(t) = -I_R(t)$, we obtain the final form of the current expression which has the same form as the Landauer formula:

$$I(t) = \frac{1}{eR_K} \int d\varepsilon T^F(\varepsilon) \{f_L^-(\varepsilon) - f_R^-(\varepsilon)\}, \quad (52)$$

where, T^F is the effective transmission probability of lead electrons thorough the island:

$$T^F(\varepsilon) = -\alpha_L^K(\varepsilon) \alpha_R^K(\varepsilon) |G_c^R(\varepsilon)|^2 \quad (53)$$

$$= -\frac{\alpha_L^K(\varepsilon) \alpha_R^K(\varepsilon)}{\alpha^K(\varepsilon)} G_c^C(\varepsilon). \quad (54)$$

From the second form, we can see our result is equivalent to that of RTA[6, 42].

In the same way as the average current, the average charge is evaluated by substitute \bar{W} into Eq. (28) [43],

$$\frac{Q(t)}{e} = \frac{1}{2} - i\hbar \left[\text{Diagram} \right],$$

where the solid dot with t corresponds to $\delta h / \delta h_\Delta(t)$ whose practical expression is equal to the right-hand side of Eq. (49) in the physical representation. The diagrammatic rule of functional derivation in terms of the scalar potential is given as follows:

(i') The diagrams corresponding to the functional derivative with respect to $h(t)$ is obtained by inserting a solid dot into all possible positions of c -field GF.

Following the rule (ii), the diagram for average charge can be also calculated:

$$\begin{aligned} \frac{Q(t)}{e} &= \frac{1}{2} + \int \frac{d\varepsilon}{2i\pi} \text{Tr} \left[\tilde{G}_c(\varepsilon) \frac{\tau^0}{2} \right] \\ &= \frac{1}{2} + \int \frac{d\varepsilon}{\pi} \frac{\alpha^R(\varepsilon)}{\alpha^K(\varepsilon)} \text{Im} G_c^R(\varepsilon). \end{aligned} \quad (55)$$

The imaginary part of G_c^R , which has a peak at $\varepsilon \sim \Delta_0$, describes the excitation property of the charge state. When the broadening of the peak is sufficiently small and $\varepsilon, T, eV \ll E_C$, G_c^R is approximately given by

$$G_c^R(\varepsilon) \sim z / (\varepsilon - z\Delta_0 + i z \text{Im} \Sigma_c^R(z\Delta_0)). \quad (56)$$

Here z is the renormalization factor $1/(1 - \partial_\varepsilon \text{Re} \Sigma_c^R(\varepsilon)|_{\varepsilon=z\Delta_0}) \sim 1/(1 + 2\alpha_0 \ln(E_C/\epsilon_C))$. The low energy cut-off ϵ_C is $\max(|z\Delta_0|, 2\pi T, |eV|/2)$ where one of three parameters must be much larger than the other two[11]. The imaginary part of self-energy $\text{Im} \Sigma_c^R$ represents the life-time broadening effect. When the renormalization effect is negligible $z \sim 1$, it is written as $\text{Im} \Sigma_c^R(z\Delta_0) \sim \gamma = \hbar\Gamma/2$, where $\Gamma = \sum_{r=L,R} (\Gamma_{Ir} + \Gamma_{rI})$ and

$$\Gamma_{rI} = \frac{\rho(\Delta_0 - \mu_r)}{e^2 R_r} n^-(\Delta_0 - \mu_r), \quad \Gamma_{Ir} = \Gamma_{rI} e^{-\beta(\Delta_0 - \mu_r)}. \quad (57)$$

Γ_{rI} (Γ_{Ir}) is equal to the tunneling rate into (out of) the island through the junction r estimated by Fermi's golden rule. It is noticed that the condition $z\alpha_0 \ll 1$ is enough to neglect the broadening of the peak. By using the approximation Eq. (56), Eq. (55) for equilibrium state reproduces the result of RTA[6], $Q/e \sim (1 - z \tanh(z\Delta_0/(2T))) / 2$.

According to Ref. [6], Eq. (52) is consistent with the co-tunneling theory and orthodox theory for two-state limit[3]. We can also confirm that Eq. (55) is consistent with the orthodox theory in the following way: In the limit of $\alpha_0 \rightarrow 0$ with keeping eV or T finite, the renormalization factor approaches unity and the imaginary part of Eq. (56) reduces to the δ -function $(-1/\pi)\delta(\varepsilon - \Delta_0)$. Thus, Eq. (55) reproduces the result of the orthodox theory

$$\lim_{\alpha_0 \rightarrow 0} Q(t)/e = \Gamma_+/\Gamma, \quad (58)$$

where $\Gamma_{+/-} = \sum_{r=L,R} \Gamma_{rI/Ir}$.

C. The current noise and the charge noise based on the reformulated resonant tunneling approximation

Here, we calculate the current noise and the charge noise based on the reformulated RTA. In the following discussions we limit ourselves to zero frequency component

$$S_{IrIr'}(0) = \int dt S_{IrIr'}(t, t'), \quad (59)$$

where we used a fact that at a stationary state, the time translational invariance is satisfied and the correlation function depends only on the difference of t and t' . From the definition Eq. (29), one obtain the current noise by applying the rule (i) twice. Reducing the number of diagrams and using the rule (ii), which can be also applied to the calculation of zero frequency noise diagram (Appendix. E), we obtain

$$\begin{aligned} \frac{S_{IrIr'}(0)}{2e^2} &= \int dt 2\text{Re} \left[\text{Diagram 1} + \text{Diagram 2} - \text{Diagram 3} \right] - \frac{(\Delta \rightarrow c)}{4} \\ &= 2 \int \frac{d\varepsilon}{h} \text{Tr} \left[\frac{\tau^0}{2} \tilde{\Sigma}_r(\varepsilon) \frac{\tau^0}{2} \tilde{G}_c(\varepsilon) \delta_{r,r'} + \frac{\tau^0}{2} \tilde{\Sigma}_r(\varepsilon) \tau^1 \tilde{G}_c(\varepsilon) \tau^1 \tilde{\Sigma}_{r'}(\varepsilon) \frac{\tau^0}{2} \tilde{G}_c(\varepsilon) - \frac{\tau^0}{2} \tilde{\Sigma}_r(\varepsilon) \tau^1 \tilde{G}_c(\varepsilon) \frac{\tau^0}{2} \tilde{\Sigma}_{r'}(\varepsilon) \tau^1 \tilde{G}_c(\varepsilon) \right] \\ &\quad - (\tau^0 \rightarrow \tau^1), \end{aligned}$$

where we used a fact that the second term of Eq. (29) is obtained from the first term by changing τ^0 to τ^1 in the physical representation (Appendix. E). After some straightforward calculations, we obtain the following expression:

$$\begin{aligned} S_{II}(0) &= S_{IrIr}(0) = -S_{IrIr}(0) \\ &= \frac{2}{R_K} \int d\varepsilon \left[-\frac{\alpha_L^K(\varepsilon)\alpha_R^K(\varepsilon)}{\alpha^K(\varepsilon)} G_c^C(\varepsilon) \{f_L^-(\varepsilon)f_R^+(\varepsilon) + f_L^+(\varepsilon)f_R^-(\varepsilon)\} - \left\{ \frac{\alpha_L^K(\varepsilon)\alpha_R^K(\varepsilon)}{\alpha^K(\varepsilon)} G_c^C(\varepsilon) \right\}^2 \{f_L^-(\varepsilon) - f_R^-(\varepsilon)\}^2 \right] \quad (60) \\ &= \frac{2}{R_K} \int d\varepsilon [T^F(\varepsilon) \{f_L^-(\varepsilon)f_R^+(\varepsilon) + f_L^+(\varepsilon)f_R^-(\varepsilon)\} - T^F(\varepsilon)^2 \{f_L^-(\varepsilon) - f_R^-(\varepsilon)\}^2], \quad (61) \end{aligned}$$

where \bar{r} is the other side of r (for example, when the index r is L the index of the other side \bar{r} is R). The charge noise is evaluated by adopting the definition Eq. (30) and by applying rules (i') and (ii):

$$\begin{aligned} S_{QQ}(0) &= e^2 \hbar^2 \int dt \left[\text{Diagram 4} \right] - \frac{(\Delta \leftrightarrow c)}{4} = e^2 \hbar^2 \int \frac{d\varepsilon}{h} \text{Tr} \left[\tilde{G}_c(\varepsilon) \frac{\tau^0}{2} \tilde{G}_c(\varepsilon) \frac{\tau^0}{2} \right] - (\tau^0 \rightarrow \tau^1) \\ &= e^2 \hbar^2 \int \frac{d\varepsilon}{h} G_c^{-+}(\varepsilon) G_c^{+-}(\varepsilon) = \sum_{r,r'=L,R} \frac{e^4 R_K}{2\pi^2} \int d\varepsilon |G_c^R(\varepsilon)|^4 \alpha_r^K(\varepsilon) \alpha_{r'}^K(\varepsilon) f_r^+(\varepsilon) f_{r'}^-(\varepsilon), \quad (62) \end{aligned}$$

where we used Eqs. (43) and (45).

Equation (61) has the same form as the current noise expression of a point contact without Coulomb interaction[44]. This result is anticipated, because the

tunneling current is expressed in the same form as the Landauer formula. However there is an important difference as mentioned in Ref. [11]: The effective transmission probability includes the Coulomb correlation and the in-

elastic relaxation effect.

Here we note the following points. First, our approximation satisfies the charge conservation law: As the approximate generating functional \bar{W} is invariant under the gauge transformation Eq. (33), we can show the conservation law, Eqs. (34) and (35), for the approximate expressions. Especially for zero frequency component, they reduce to equations for the current conservation law, $\sum_{r=L,R} I_r = 0$ and $\sum_{r,r'=L,R} S_{I_r I_{r'}}(0) = 0$. It is worth noticing that the gauge invariance is automatically satisfied when \bar{W} consists of closed diagrams. Secondly, we can show that our result satisfies the fluctuation-dissipation theorem: At $V = 0$, the current noise expression is reduced to the Johnson-Nyquist formula $S_{II}(0) = 4T\bar{G}$, where \bar{G} is the conductance expressed as $\bar{G} = \lim_{V \rightarrow 0} \partial I / \partial V = R_K^{-1} \int d\varepsilon T^F(\varepsilon) / \{4T \cosh(\varepsilon/(2T))\}^2$.

We discuss the current noise expression in the regime where $z\alpha_0 \ll 1$ and the renormalization effect is negligible, $z \sim 1$. Using Eqs. (53) and (56), the first term of Eq. (60) is approximately given by

$$2e(\gamma_r^+(\gamma) + \gamma_r^-(\gamma)), \quad (63)$$

where

$$\begin{aligned} \gamma_r^+(\gamma) &= \frac{R_K}{4\pi^2 e R_L R_R} \int d\varepsilon \frac{\rho(\varepsilon - \mu_r) n_r^-(\varepsilon) \rho(\varepsilon - \mu_{\bar{r}}) n_{\bar{r}}^+(\varepsilon)}{|\varepsilon + i\gamma - \Delta_0|^2}, \\ \gamma_r^-(\gamma) &= \gamma_r^+(\gamma) e^{-\beta eV}. \end{aligned} \quad (64)$$

For $\gamma = 0$, $\gamma_r^{+/-}(0)$ is the co-tunneling current from lead r/\bar{r} to lead \bar{r}/r , and Eq. (63) reproduces the co-tunneling theory [14, 20, 21] in the two-state limit. Equation (63), which we call the *co-tunneling theory with life-time broadening*, is equivalent to the previously proposed equation in Ref. [13] in the limit of $T \rightarrow 0$. The validity of this approximation is discussed in the next section from the point of view of the numerical results.

By taking the limit $\alpha_0 \rightarrow 0$, with paying attention to the relation $\lim_{\gamma \rightarrow 0} (2\pi\gamma) \{ \text{Im}[1/(\varepsilon - \Delta_0 + i\gamma)] \}^2 = \delta(\varepsilon - \Delta_0)$, we obtain the result of the orthodox theory in the two-state limit:

$$\lim_{\alpha_0 \rightarrow 0} [\alpha_0^{-1} S_{II}(0)] = \alpha_0^{-1} 2e \left(I_+ - \frac{2I_-^2}{e\Gamma} \right), \quad (65)$$

where $I_{\pm} = e(\Gamma_{LI}\Gamma_{IR} \pm \Gamma_{IL}\Gamma_{RI})/\Gamma$. I_- is the average current of the orthodox theory. The second term is related to the part of Eq. (60) proportional to $(T^F)^2$, which represents the Coulomb correlation and reduces the current noise from the Poissonian value. It is noticed that even at small tunneling conductance, the second term is important in ST regime.

In the same way as above discussions, for $z\alpha_0 \ll 1$ and $z \sim 1$, we obtain the co-tunneling theory[14] with life-time broadening from Eq. (62):

$$S_{QQ}(0) \sim \sum_{r,r'=L,R} \frac{e^4 R_K}{2\pi^2} \int d\varepsilon \frac{\alpha_r^K(\varepsilon) \alpha_{r'}^K(\varepsilon) f_r^+(\varepsilon) f_{r'}^-(\varepsilon)}{\{(\varepsilon - \Delta_0)^2 + \gamma^2\}^2}. \quad (66)$$

In the limit of $\alpha_0 \rightarrow 0$, we can confirm that our result reproduces the orthodox theory[45]:

$$\lim_{\alpha_0 \rightarrow 0} [\alpha_0 S_{QQ}(0)] = \alpha_0 4e^2 \Gamma_+ \Gamma_- / \Gamma^3. \quad (67)$$

IV. RESULTS AND DISCUSSIONS

In this section we present results obtained by the numerical calculation of Eqs. (60) and (62)[46], based on which we discuss the non-equilibrium fluctuation in Sec. IV A and that of thermal fluctuation in Sec. IV B. We also discuss the effect of renormalization on the noise at low temperature caused by quantum fluctuation in Sec. IV C.

A. Noise in the non-equilibrium state

In order to clarify the nature of non-equilibrium current fluctuation, we consider the case of zero temperature, where there is no thermal fluctuation. Furthermore, we limit ourselves to the condition of the high bias voltage, $E_C \gg |eV| \gg T_K$, where the renormalization effect is negligible. Figure 5 shows the current noise (the top panel) and the charge noise (the bottom panel) as a function of the excitation energy Δ_0 for small α_0 ((a-1) and (b-1)) and those for large α_0 ((a-2) and (b-2)). Plots are normalized by values of the orthodox theory at $\Delta_0 = 0$. Solid lines, dashed lines and dotted lines show results of our approximation (Eqs. (60) and (62)), the orthodox theory (Eqs. (65) and (67)) and the co-tunneling theory (Eqs. (63) and (66) with $\gamma = 0$), respectively.

When α_0 is small, our results well reproduce the orthodox theory ((a-1) and (b-1)). For large α_0 ((a-2) and (b-2)) and in CB regime ($|\Delta_0/(eV)| \gg 0.5$), they agree well with the co-tunneling theory. Figure 6 shows the average current (a) and the average charge (b) estimated by our approximation (solid lines) and the orthodox theory (dashed lines). In CB regime, we can see both the average value and the noise are enhanced by the quantum fluctuation. Around $\Delta_0 = 0$, the average current and the current noise are strongly suppressed due to the life-time broadening effect [6].

Next, we discuss the validity of the co-tunneling theory with life-time broadening (see Eqs. (63) and (66); dot-dashed lines in Fig. 5). As for the charge noise in the limit of $\alpha_0 \rightarrow 0$, it reproduces the result of the orthodox theory as well as our approximation (Fig. 5 (b-1): The solid line and the dot-dashed line almost overlap each other). In ST regime it overestimates the current noise (Fig. 5 (a-1)), because it does not take the Coulomb correlation effect into account as mentioned before. We want to stress again that our result reproduces the orthodox theory in the limit of $\alpha_0 \rightarrow 0$, which can not be achieved by the co-tunneling theory with life-time broadening.

The physical picture of the non-equilibrium current fluctuation is understood more clearly with the help of

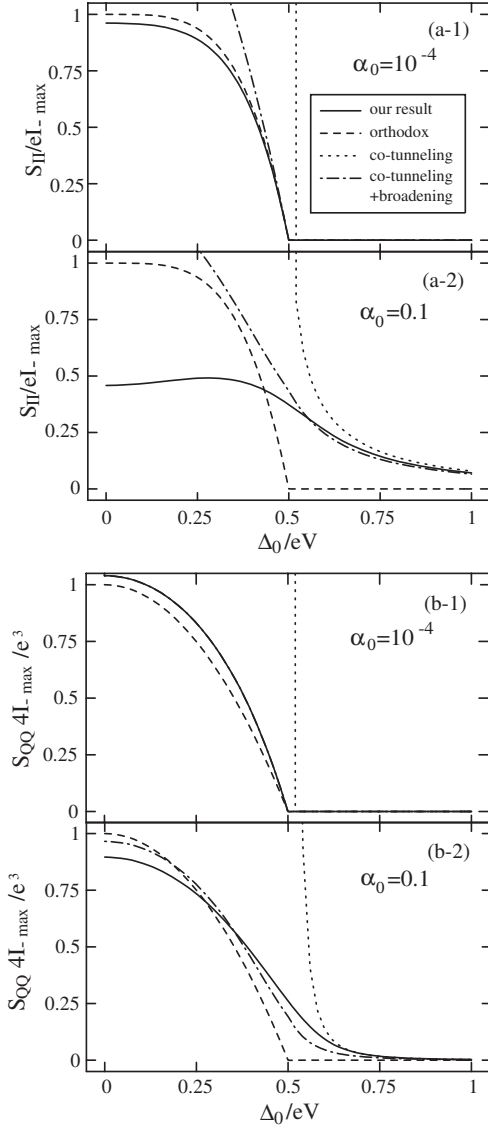


FIG. 5: The excitation energy dependence of the current noise (the top panel) and the charge noise (the bottom panel) for $\alpha_0 = 10^{-4}$ ((a-1) and (b-1)) and 0.1 ((a-2) and (b-2)) at 0K and $eV/E_C = 0.4$. Plots are normalized by the value predicted by the orthodox theory at $\Delta_0 = 0$: $eI_{-max} = eG_0V/2$ for the current noise and $e^3/(4I_{-max})$ for the charge noise, where $G_0 = 1/(R_L + R_R)$ is the series junction conductance. The solid, dashed, dotted and dot-dashed lines show the results evaluated by our approximation, orthodox theory, co-tunneling theory and co-tunneling theory with lifetime broadening, respectively. In the panel (b-1), the solid line and dot-dashed line almost overlap each other. The parameters satisfy $eV \gg T_K$; For example, $T_K/E_C \sim 10^{-3}$ for $\alpha_0 = 0.1$.

the Fano factor defined by $S_{II}/(2eI)$. The Fano factor is unity when the tunneling event of electrons is Poissonian process and is suppressed when tunneling events are correlated. The orthodox theory predicts the sub-Poissonian behavior in ST regime because of the Coulomb cor-

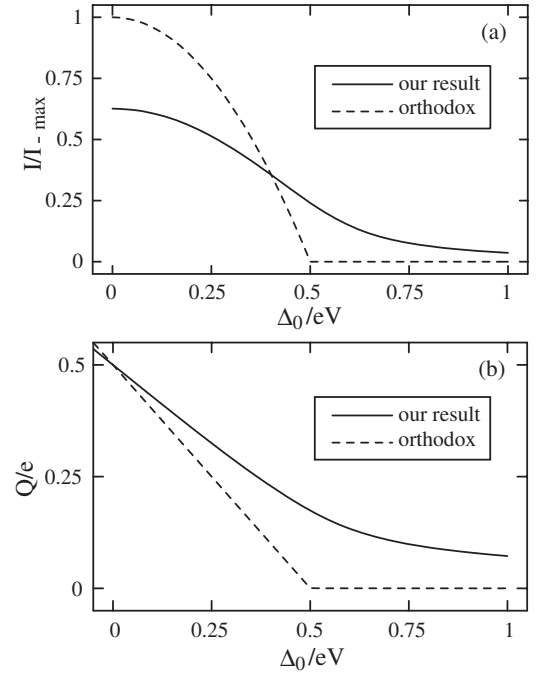


FIG. 6: The excitation energy dependence of the normalized average current (a) and the average charge (b) for $\alpha_0 = 0.1$ at 0K and $eV/E_C = 0.4$. The solid and dashed lines show the results of ours and those of orthodox theory, respectively.

relation: Suppose one electron tunnels into the island through one junction, the next tunneling event must be the out going process of another electron through the other junction. In CB regime, the co-tunneling theory predict $S_{II}/(2eI) = 1$. It means that co-tunneling events, viz. the simultaneous tunneling events of two electrons through the two junctions, occur randomly.

The figure 7 shows the excitation energy dependence of the Fano factor obtained by our approximation. In the small α_0 limit, our approximation reproduces the orthodox theory in ST regime and the co-tunneling theory in CB regime and smoothly interpolate two theories (The dotted line actually almost coincides with the result of orthodox theory in ST regime). For larger α_0 the Fano factor is further suppressed (the dashed and the solid line). Especially, our result predicts the value smaller than 1/2 at the degeneracy point. It is a distinctive result because the orthodox theory predicts the inequality $S_{II}/(2eI) \geq 1/2$ (p. 137 in Ref. [12]).

Next we consider the physical meaning of our result. In CB regime and near the threshold voltage, the origin of the suppression of Fano factor is considered to be the enhancement of the effective transmission probability T^F , because the increase in the current noise is much larger than that in the charge noise (see Figs. 5 (a-2) and 5 (b-2)). As the Fano factor of the shot noise is approximately given by $1 - T^F$ [12], the enhancement of the transmission probability results in the suppression of the Fano factor.

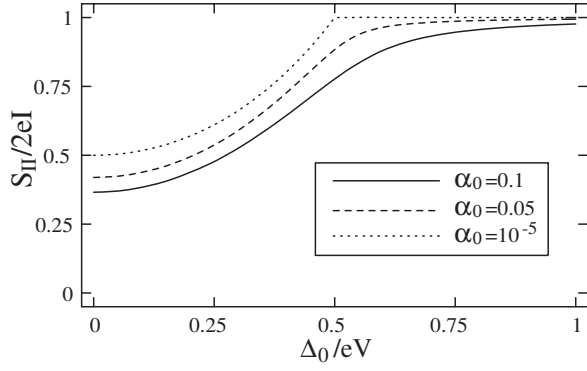


FIG. 7: The excitation energy dependence of the Fano factor at $eV/E_C = 0.4$ for $\alpha_0 = 10^{-5}$ (dotted line), 0.05 (dashed line) and 0.1 (solid line).

Around the degeneracy point, the origin of the suppression of Fano factor is different, because the normalized current and the current noise are suppressed as shown in Fig. 6 (a) and Fig. 5 (a-2). We consider that the Fano factor is suppressed because of the dissipation, i.e. the life-time broadening effect: RTA takes account of the dissipation process which is the leak of an electron from the island while another electron tunnels into the island and relaxes to the local equilibrium state of the island. The suppression of the Fano factor by the dissipation was previously predicted for the 1D electron channel coupled with a boson bath[47, 48].

B. Effect of thermal fluctuation

Next we discuss the effect of the thermal fluctuation. Figure 8 shows the temperature dependence of the current noise (a), the average current (b) and the Fano factor (c) at a threshold for various α_0 . They are normalized by the value of the orthodox theory at $T = \Delta_0 = 0$.

As the temperature increases, the average current and the current noise increase because of the thermal fluctuation. At sufficiently high temperature $E_C \gg T \gg |eV|/2$, orthodox theory predicts that the average current saturates at I_{max} and the thermal fluctuation dominates the current noise, i.e. $S_{II} \sim 4(G_0/2)T$ which is the similar form as the Johnson-Nyquist noise for the ohmic resistance[37] (the plot for $\alpha_0 = 10^{-5}$ almost coincides with the orthodox theory). Our result further shows that the average current and the current noise are suppressed as α_0 increases (panels (a) and (b)). It is considered to be attributed to the higher order tunneling effect: The lifetime broadening caused by the thermal fluctuation is enhanced for the large tunnel conductance. The panel (c) is the Fano factor versus temperature plot. The Fano factor is independent of α_0 , which means that the correlation between tunneling events does not depend on α_0 .

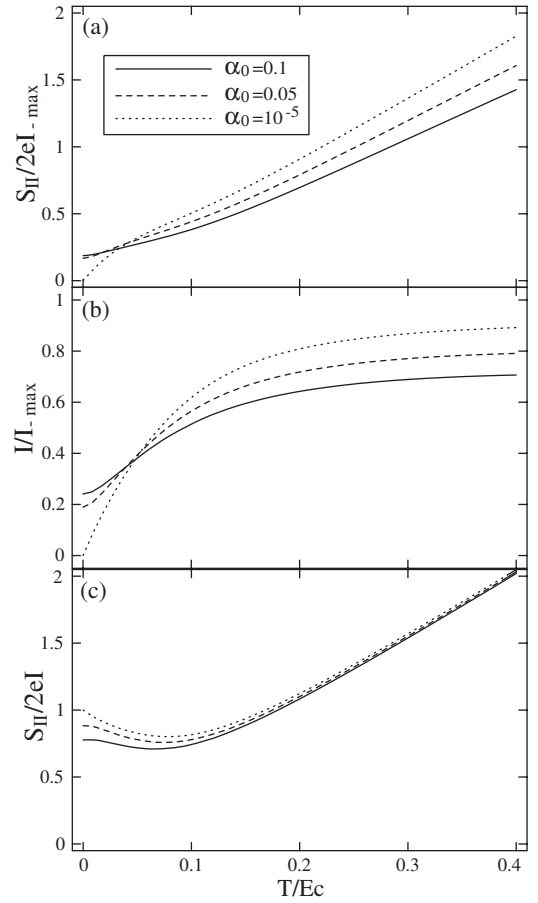


FIG. 8: The temperature dependence of the normalized current noise (a) and the normalized average current (b) at a threshold $eV/2 = \Delta_0 = 0.2E_C$ for $\alpha_0 = 10^{-5}$ (dotted line), 0.05 (dashed line) and 0.1 (solid line). (c) The temperature dependence of the Fano factor for various α_0 at the threshold.

C. Renormalization effect

Next we consider the renormalization effect at low bias voltage and temperature: $eV, T \lesssim T_K$. Figures 9 (a) and (b) show the charge noise normalized by $e^4 R_T/E_C$ at $\Delta_0 = 0$ as a function of the temperature and the bias voltage, respectively. The charge noise is suppressed for large α_0 , which is attributed to the renormalization of the system parameters. In the regime $eV, T \ll T_K$, where the life-time broadening effect is negligible ($z\alpha_0 \ll 1$), we can approximate Eq. (62) as

$$4(z e)^2 \tilde{\Gamma}_+ \tilde{\Gamma}_- / \tilde{\Gamma}^3, \quad (68)$$

instead of Eq. (67). Here $\tilde{\Gamma}$ and $\tilde{\Gamma}_{\pm}$ are tunneling rate Eq. (57) written by using renormalized parameters such as $\tilde{\Gamma}_{rI} = z \rho(z \Delta_0 - \mu_r) n^-(z \Delta_0 - \mu_r) / (e^2 R_r)$ where the renormalization factor z is $1/(1 + 2\alpha_0 \ln(E_C/\epsilon_C))$. The lower cut-off energy ϵ_C is $2\pi T$ for the panel (a) and $|eV|/2$ for the panel (b). It is natural to interpret Eq. (68) that the charge of a carrier is modified as $z e$ by

the renormalization effect. The interpretation is similar to that of the doubling of shot noise at the normal-metal(N)-superconductor(S) interface. Since at NS interface the carrier is $2e$ -charged particle, viz. a Cooper pair, the shot noise is twice as large as that at NN interface [49].

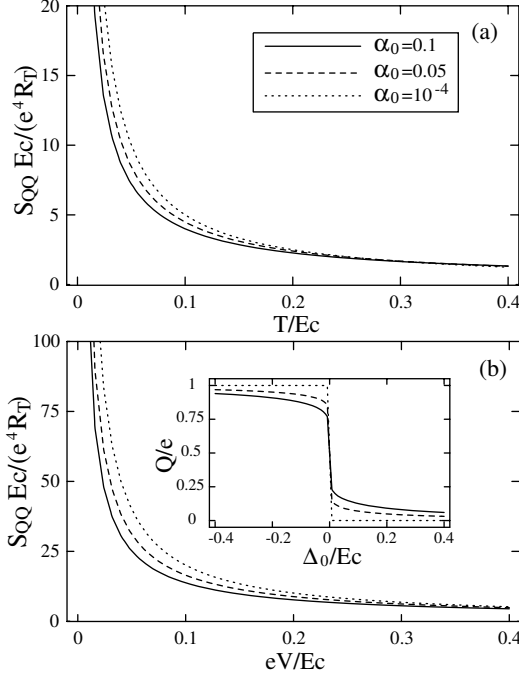


FIG. 9: (a) The normalized charge noise as a function of temperature at $\Delta_0 = eV = 0$ for $\alpha_0 = 0.1$ (solid line), 0.05 (dashed line) and 10^{-4} (dotted line). (b) The normalized charge noise as a function of bias voltage at $\Delta_0 = T = 0$. Inset: The average charge as a function of Δ_0 at $T = eV = 0$.

Though the normalized charge noise is suppressed with increasing α_0 , one sees that the charge noise always diverges at $\Delta_0 = T = eV = 0$ for arbitrary α_0 in the weak tunneling regime. Since the charge noise is related to the “charge susceptibility” for excitation energy Δ_0 , the divergence means that the number of charge changes by “one” at the degeneracy point when we sweep the excitation energy. It is confirmed by the fact that the slope of excitation energy dependence of the average charge (an inset of Fig. 9 (b)) diverges at the degeneracy point.

Next we discuss the renormalization effect on the Fano factor. Figure 10 shows the excitation energy dependence of the Fano factor for various bias voltage. We can see at small bias voltage where the charging energy renormalization is pronounced $|eV| \lesssim T_K \sim 10^{-3}$, the valley structures of curves are widened. The same behavior can be seen in the differential conductance shown in Refs. [3, 8, 11]. We also see that the Fano factor is suppressed with increasing bias voltage at $\Delta_0 = 0$. This suppression is also attributed to the dissipation as discussed in Sec. IV A: As the bias voltage increases, the dissipative charge fluctuation is enhanced and thus the Fano factor

is suppressed.

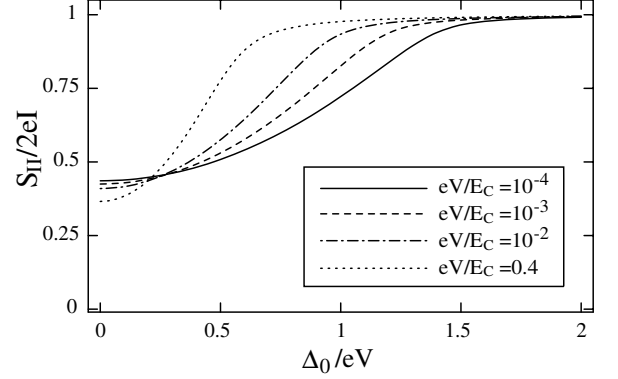


FIG. 10: The excitation energy dependence of the Fano factor for $\alpha_0 = 0.1$ at $eV/E_C = 10^{-4}$ (solid line), 10^{-3} (dashed line), 10^{-2} (dot-dashed line) and 0.4 (dotted line).

V. SUMMARY

By using the drone-fermion representation and the Schwinger-Keldysh approach, we have calculated the current noise and the charge noise in the regime of large quantum fluctuations of charge out of equilibrium. We have reformulated and extended RTA in a charge conserving way. Our approximation interpolates previous theories, the orthodox theory and the co-tunneling theory: Our result coincides with the orthodox theory in the limit of $\alpha_0 \rightarrow 0$ and is consistent with the co-tunneling theory in CB regime. The approximation is verified from the fact that the result satisfies the fluctuation-dissipation theorem. In previous papers, we also checked numerically that the energy sensitivity does not exceed the quantum limit [50, 51].

We showed that at zero temperature and $E_C \gg |eV| \gg T_K$, the life-time broadening caused by non-equilibrium dissipative charge fluctuation suppresses the current noise in ST regime. It also suppresses the Fano factor more than the Coulomb correlation does. Especially the Fano factor is suppressed below the minimum value predicted by the orthodox theory $1/2$ around $\Delta_0 = 0$. The origin of the suppression is attributed to the charge fluctuation which appears as the enhancement of the transmission probability in CB regime and the dissipation in ST regime.

At $E_C \gg T \gg |eV|/2 \gg T_K$, we showed that the average current and the current noise deviate from the predictions of the orthodox theory with increasing α_0 . However, the Fano factor is independent of α_0 and is proportional to the temperature. It means that the current noise is dominated by the thermal fluctuation and the correlation between the tunneling events does not depend on α_0 .

At small bias voltage and temperature $eV, T \lesssim T_K$, the charge noise is suppressed as compared with the predic-

tion of the orthodox theory. We showed that it can be interpreted as the renormalization for the unit of island charge. Although the charge is renormalized, the charge noise diverges at $\Delta_0 = T = eV = 0$ for arbitrary α_0 in the weak tunneling regime. It means that the quantum fluctuation does not wash out the charge quantization.

In this paper, we have limited ourselves to the discussions on the second moment and the zero frequency component, because we think them primitive. The investigation on the frequency dependence of noise will be important to estimate the performance of high-speed SET electrometer completely[15]. The investigation on the higher order moment and the full counting statistics[52, 53] will help us to understand carriers of strongly correlated system out of equilibrium.

Acknowledgments

We would like to thank Y. Isawa, J. Martinek, Yu. V. Nazarov and G. Johansson for variable discussions and comments. This work was supported by a Grant-in-Aid for Scientific Research (C), No. 14540321 from MEXT. H.I. was supported by MEXT, Grant-in-Aid for Encouragement of Young Scientists, No. 13740197.

APPENDIX A: RELATION BETWEEN GENERATING FUNCTIONAL REPRESENTATION AND OPERATOR REPRESENTATION

In this Appendix, we show the relation between expressions for average and noise in the operator representation and those in the generating functional representation. The variation of the exact action Eq. (15) accompanied by the infinitesimal variation of h is given as the “twisted” combination (Sec. 9.3.2 in Ref. [25]) of Q and h ,

$$\delta S = - \int dt \frac{Q_c(t)}{e} \delta h_\Delta(t) + (c \leftrightarrow \Delta), \quad (\text{A1})$$

where the center-of-mass coordinate of charge is $Q_c(t) = e(c_+(t)^*c_+(t) + c_-(t)^*c_-(t))/2$. Employing this source term, we can show that the Eq. (28) is equivalent to $\langle \hat{Q}(t) \rangle$ where $\hat{Q} = e(\hat{\sigma}_z + 1)/2 = e\hat{c}^\dagger\hat{c}$:

$$-e \left. \frac{\delta W}{\delta h_\Delta(t)} \right| = \langle Q_c(t) \rangle = \langle \hat{Q}(t) \rangle - \frac{e}{2},$$

where we used Eq. (9) to obtain the final form.

The second derivative $-i\hbar e^2 \delta^2 W / \delta h_\Delta(t) \delta h_\Delta(t')$ is calculated as

$$\{ \langle Q_c(t) Q_c(t') \rangle - \langle Q_c(t) \rangle \langle Q_c(t') \rangle \}. \quad (\text{A2})$$

Here the first term includes the correlation function of 4 field variables on a same branch, $\langle c_\pm^*(t) c_\pm(t) c_\pm^*(t') c_\pm(t') \rangle$,

which is not well defined at $t = t'$. Usually, an additional operation to determine the order of field variables is required to remove the uncertainty. Alternatively, we subtract a term

$$\frac{1}{4} \left. \frac{-i\hbar e^2 \delta^2 W}{\delta h_c(t) \delta h_c(t')} \right| = \frac{\langle Q_\Delta(t) Q_\Delta(t') \rangle}{4}, \quad (\text{A3})$$

from Eq. (A2) as shown in our definition Eq. (30). Here we used the normalization Eq. (11), $\langle Q_\Delta(t) \rangle = 0$. As a result, the first term in Eq. (A2) is replaced by $(\langle Q_+(t) Q_-(t') + Q_-(t) Q_+(t') \rangle)/2$, which does not include the uncertainty. Using Eq. (9), we show that our definition is equal to the standard charge noise expression

$$\left. \frac{-i\hbar e^2 \delta^2 W}{\delta h_\Delta(t) \delta h_\Delta(t')} \right| - \frac{(\Delta \rightarrow c)}{4} = \langle \{ \delta \hat{Q}(t), \delta \hat{Q}(t') \} \rangle.$$

We should stress that our definition does not change the final result because Eq. (A3) is 0 from the normalization.

The exact current expression is obtained in the same way. The source term corresponding to Eq. (A1) is given by $\delta S = (\hbar/e) \int dt \sum_{r=L,R} I_{rc}(t) \delta \varphi_{r\Delta}(t) + (c \leftrightarrow \Delta)$, which leads to relations

$$I_r(t) = \langle \hat{I}_r(t) \rangle, \quad S_{I_r I_{r'}}(t, t') = \langle \{ \delta \hat{I}_r(t), \delta \hat{I}_{r'}(t') \} \rangle,$$

where the current operator at junction r is defined as $\hat{I}_r(t) = (ie/\hbar) \sum_{kn} T_r e^{i\varphi_r(t)} \hat{a}_{1kn}^\dagger \hat{a}_{rkn} \hat{\sigma}_+ + \text{h.c.}$

APPENDIX B: CHARGE CONSERVATION

In this Appendix, we demonstrate the charge conservation law. As W is invariant under the transformation Eq. (33), we obtain an identity

$$-e \partial_t \delta W / \delta h_\Delta(t) = (e/\hbar) \sum_{r=L,R} \delta W / \delta \varphi_{r\Delta}(t). \quad (\text{B1})$$

We can derive the other equation, which is obtained from above equation by replacing Δ with c . However, the latter equation is not important in the following discussions. By putting the auxiliary source fields as the values given in the subscripts of Eq. (27), and employing Eqs. (27) and (28), we obtain the current continuity equation, Eq. (34).

Next we demonstrate the charge conservation law for correlation functions. By acting the operator $ie\hbar \partial_{t'} \delta / \delta h_\Delta(t')$ or $-ie \sum_{r'=L,R} \delta / \delta \varphi_{r\Delta}(t')$ on Eq. (B1), we obtain following two equations:

$$\begin{aligned} -\partial_{t'} \partial_t \frac{i\hbar e^2 \delta^2 W}{\delta h_\Delta(t') \delta h_\Delta(t)} &= \partial_{t'} \sum_{r=L,R} \frac{ie^2 \delta^2 W}{\delta h_\Delta(t') \delta \varphi_{r\Delta}(t)}, \\ \partial_t \sum_{r'=L,R} \frac{ie^2 \delta^2 W}{\delta \varphi_{r'\Delta}(t') \delta h_\Delta(t)} &= \sum_{r,r'=L,R} \frac{e^2}{i\hbar} \frac{\delta^2 W}{\delta \varphi_{r'\Delta}(t') \delta \varphi_{r\Delta}(t)}. \end{aligned}$$

By comparing the left-hand side of the former equation and the right-hand side of the latter equation, by setting

the auxiliary source fields as the values given in the subscripts of Eq. (27), and by using Eqs. (29) and (30), we obtain the charge conservation law for correlation functions, Eq. (35).

APPENDIX C: LOOP DIAGRAMS: PARTICLE-HOLE GREEN FUNCTION AND SELF-ENERGY

In this Appendix, we calculate the particle-hole GF. We begin with the tunneling action for the large transverse channel obtained from Eq. (15) by tracing out the electron degrees of freedom[36]: $S_T = \int_C d1 d2 \sigma_+(1) \alpha(1, 2) \sigma_-(2)$. In the physical representation, it is rewritten as $\int d1 d2 \tilde{\sigma}_+(1)^\dagger \tau^1 \tilde{\alpha}_r(1, 2) \tau^1 \tilde{\sigma}_-(2)$, where the vector field $\tilde{\sigma}_\pm$ is defined in the same way as Eq. (6). Each component of $\tilde{\alpha}_r$ can be calculated by utilizing the functional derivation. For example, (1,2)-component is

$$\begin{aligned} (\tau^1 \tilde{\alpha}_r(1, 2) \tau^1)_{1,2} &= \frac{\delta^2 S_T}{\delta \sigma_{+1}(1)^* \delta \sigma_{-2}(2)} \\ &= -i\hbar N_{\text{ch}} T_r^2 \text{Tr} \left[\frac{\delta \sigma_+^*}{\delta \sigma_{+1}(1)^*} e^{i\varphi_r} g_r \frac{\delta \sigma_-}{\delta \sigma_{-2}(2)} e^{i\varphi_r} g_l \right]. \end{aligned} \quad (\text{C1})$$

As the functional derivative is $\delta \tilde{\sigma}_\pm(t')/\delta \sigma_{\pm 1(2)}(t) = \tau^{0(1)} \delta(t-t')/\sqrt{2}$ in the physical representation, the trace yields $e^{i\kappa_r eV(t_2-t_1)/\hbar} \text{Tr}[\tau^0 \tilde{g}_r(1, 2) \tau^1 \tilde{g}_l(2, 1)]/2$. Here we put $\varphi_\Delta = 0$ and $\varphi_c(t) = eVt/\hbar$. The other components

are evaluated in the same way. Then four components are given as

$$\begin{pmatrix} 0 & g_r^A g_l^K + g_r^K g_l^R \\ g_r^R g_l^K + g_r^K g_l^A & g_r^K g_l^K - g_r^C g_l^C \end{pmatrix}, \quad (\text{C2})$$

where we omitted arguments and coefficients. To obtain this form, we used the normalization Eq. (11) or the relation $\theta(t)\theta(-t) = 0$ (see Eqs. (2.64) and (2.65) in Ref. [25]). The following calculations are same as those in Ref. [36]. Employing the Fourier transforms of the GF defined in Eq. (18), $g_r^K(\varepsilon) = -i\pi\rho_r(\varepsilon)$ and $g_r^K(\varepsilon) = -2i\pi\rho_r(\varepsilon) \tanh(\varepsilon/(2T))$, we obtain Eq. (39).

Another loop diagram, the self-energy Eq. (24), can be calculated in the same way. Four components are given in the same form as those of Eq. (C2). By using Eqs. (36) and (39), we obtain

$$\Sigma_r^R(\varepsilon) = \int \frac{d\varepsilon'}{2\pi} \frac{i\alpha_r^K(\varepsilon')}{\varepsilon + i\eta - \varepsilon'}, \quad \Sigma_r^K(\varepsilon) = \alpha_r^C(\varepsilon).$$

From these equations, Eqs. (40) and (41) can be derived.

APPENDIX D: PERTURBATION THEORY

In this Appendix, we describe some results of finite order perturbation theory and explain why we introduced Eq. (25) which takes account of all orders for c -field corrections. First, we calculate the first order contribution of average charge by employing $W^{(1)}$, Eq. (28) and rules (i') and (ii).

$$\begin{aligned} \frac{Q^{(1)}(t)}{e} &= -i\hbar \left(\text{Diagram: a circle with a dot and a line labeled 't' entering from the left} \right) = -\frac{i}{2\pi} \int d\varepsilon \text{Tr} \left[\frac{\tau^0}{2} \tilde{g}_c(\varepsilon) \tau^1 \tilde{\Sigma}_c(\varepsilon) \tau^1 \tilde{g}_c(\varepsilon) \right] \\ &= -i \int \frac{d\varepsilon}{8\pi} (g_c^K(\varepsilon) g_c^P(\varepsilon) \Sigma_c^P(\varepsilon) + g_c^K(\varepsilon) g_c^C(\varepsilon) \Sigma_c^C(\varepsilon) + 2|g_c^R(\varepsilon)|^2 \Sigma_c^K(\varepsilon)), \end{aligned}$$

where GF denoted with superscript P is given as $g_c^P = g_c^R + g_c^A$ etc. In the equilibrium state, the second and the third terms of the second line are negligibly small $O(\Delta_0/E_C)$ and the first term is simplified to

$$\frac{Q^{(1)}}{e} \sim \frac{1}{2} \partial_{\Delta_0} \left\{ \tanh\left(\frac{\Delta_0}{2T}\right) \text{Re} \Sigma_c^R(\Delta_0) \right\}, \quad (\text{D1})$$

where we utilized the relation $g_c^K(\varepsilon) g_c^P(\varepsilon) = \partial_{\Delta_0} g_c^K(\varepsilon)$. In the limit of zero temperature, Eq. (D1) leads to the log-divergence[3, 4] as $\sim -\alpha_0 \ln(E_C/|\Delta_0|) \text{sgn}(\Delta_0)$.

Above result suggests that the c -field correction is responsible for the divergence. It is further confirmed by calculating second order contribution of average current

generated from c -field correction $W_{c\text{-field}}^{(2)}$. Employing rules (i) and (ii), we obtain

$$\begin{aligned} I_r^{(2)}(t) &= 2e \text{Re} \left(\text{Diagram: a circle with a dot and a line labeled 't' entering from the left, and a line labeled 't' entering from the right} \right) \\ &= 2e \text{Re} \int \frac{d\varepsilon}{h} \text{Tr} \left[\frac{\tau^0}{2} \tilde{\Sigma}_r(\varepsilon) \tau^1 \tilde{g}_c(\varepsilon) \tau^1 \tilde{\Sigma}_c(\varepsilon) \tau^1 \tilde{g}_c(\varepsilon) \right] \\ &= e \int \frac{d\varepsilon}{2h} |g_c^R(\varepsilon)|^2 \Sigma_r^K(\varepsilon) \Sigma_r^C(\varepsilon) - (C \leftrightarrow K) + \delta I_r^{(2)} \\ &= \gamma_r^+(\eta) - \gamma_r^-(\eta) + \delta I_r^{(2)}. \end{aligned} \quad (\text{D2})$$

The first and the second terms of Eq. (D2), which are consistent of the expression for co-tunneling current

[22], also diverge at the degeneracy point. From above discussions, we can deduce that the most simple way to regulate the divergence is to sum up c -field corrections $(g_c \Sigma_c)^n$ up to infinite n as shown in Eq. (25). It should be noted that the correction term $\delta I_r^{(2)} = e \int d\varepsilon g_c^C(\varepsilon) \Sigma_r^C(\varepsilon) \{g_c^C(\varepsilon) \Sigma_r^K(\varepsilon) - g_c^K(\varepsilon) \Sigma_c^C(\varepsilon)\} / (4h) \sim O(1/\eta)$ diverges in the limit of $\eta \rightarrow 0$. This divergence disappears when we consider Eq. (25) as discussed in Sec. IIIB and Sec. IIIC.

APPENDIX E: RULE FOR CALCULATION OF ZERO FREQUENCY NOISE DIAGRAMS

In this Appendix, we demonstrate that the rule (ii) can be also applied to the calculation of zero-frequency noise. We also demonstrate the rule to calculate the second term of the noise expression Eq. (29) or Eq. (30). For example, we consider the current noise related to $W^{(1)}$. Though we consider the simple case, the following discussions can be generalized. From the definition Eq. (32), the noise diagrams is obtained as:

$$\frac{S_{IrIr'}^{(1)}(0)}{2e^2} = \int dt 2\text{Re} \left[\text{Diagram} \right] \delta_{r,r'} - \frac{(\Delta \rightarrow c)}{4}. \quad (\text{E1})$$

The integration in terms of t in the first term is calculated as

$$\begin{aligned} \int dt \left[\text{Diagram} \right] &= \int dt \text{Tr} \left[\frac{\delta \varphi_r}{\delta \varphi_{r\Delta}(t)} \Sigma_r \frac{\delta \varphi_{r'}}{\delta \varphi_{r'\Delta}(t')} g_c \right] \\ &= \int \frac{d\varepsilon}{h} \text{Tr} \left[\frac{\tau^0}{2} \tilde{\Sigma}_r(\varepsilon) \frac{\tau^0}{2} \tilde{g}_c(\varepsilon) \right]. \end{aligned} \quad (\text{E2})$$

And thus we can see that the rule (ii) can be applied for the calculation of the zero-frequency current noise. As for the second term, the derivation

$$\delta \tilde{\varphi}_r(t') / \delta \varphi_{rc}(t) = \tau^1 \delta(t - t'), \quad (\text{E3})$$

appears instead of Eq. (49). Thus we can derive the rule that the second term is obtained from the first term by replacing τ^0 with τ^1 as $\int d\varepsilon 2\text{ReTr} \left[(\tau^1/2) \tilde{\Sigma}_r(\varepsilon) (\tau^1/2) \tilde{g}_c(\varepsilon) \right] / h$ [54]. As a result, Eq. (E1) is expressed as

$$\text{Re} \int d\varepsilon \text{Tr} \left[\tau^0 \tilde{\Sigma}_r(\varepsilon) \tau^0 \tilde{g}_c(\varepsilon) \right] \delta_{r,r'} / (2h) - (\tau^0 \rightarrow \tau^1).$$

As for the charge noise, we can repeat the same discussions as above.

-
- [1] D. V. Averin and K. K. Likharev, in *Mesoscopic Phenomena in Solids*, edited by B. L. Altshuler, P. A. Lee, and R. A. Webb (Elsevier Science Publishers B. V., Amsterdam, 1991), vol. 30 of *Modern Problem in Condensed Matter Sciences*, chap. 6.
 - [2] G.-L. Ingold and Y. V. Nazarov, in [55], chap. 2, p. 21.
 - [3] G. Schön, in *Quantum Transport and Dissipation*, edited by T. Dittrich, P. Hänggi, G.-L. Ingold, B. Kramer, G. Schön, and W. Zwerger (Wiley-VCH, Weinheim, 1998), p. 149.
 - [4] K. A. Matveev, Sov. Phys. JETP. **72**, 892 (1991).
 - [5] G. Falci, G. Schön, and G. T. Zimanyi, Phys. Rev. Lett. **74**, 3257 (1995).
 - [6] H. Schoeller and G. Schön, Phys. Rev. B **50**, 18436 (1994).
 - [7] H. Schoeller and J. König, Phys. Rev. Lett. **84**, 3686 (2000).
 - [8] J. König, H. Schoeller, G. Schön, and R. Fazio, in *Quantum Dynamics of Submicron Structures*, edited by H. A. Cerdeira, B. Kramer, and G. Schön (Kluwer Academic Publishers, Dordrecht, 1995), vol. 291 of *NATO ASI Series E*, p. 221, and references therein.
 - [9] D. S. Golubev and A. D. Zaikin, Phys. Rev. B **50**, 8736 (1994).
 - [10] P. Joyez, V. Bouchiat, D. Esteve, C. Urbina, and M. H. Devoret, Phys. Rev. Lett. **79**, 1349 (1997).
 - [11] H. Schoeller, in *Mesoscopic Electron Transport*, edited by L. L. Sohn, L. P. Kouwenhoven, and G. Schön (Kluwer Academic Publishers, Dordrecht, 1997), vol. 345 of *NATO ASI Series E*, p. 291.
 - [12] Y. M. Blanter and M. Buttiker, Phys. Rep. **336**, 1 (2000).
 - [13] A. N. Korotkov, D. V. Averin, K. K. Likharev, and S. A. Vasenko, in *Single-Electron Tunneling and Mesoscopic Devices*, edited by H. Koch and H. Lübbig (Springer-Verlag, Berlin, 1992), vol. 31 of *Springer Series in Electronics and Photonics*, pp. 45–59.
 - [14] D. V. Averin, in *Macroscopic Quantum Coherence and Quantum Computing*, edited by D. V. Averin, R. Ruggerio, and P. Silvestrini (Kluwer Academic/Plenum Publishers, New York, 2001), pp. 399–407.
 - [15] G. Johansson, A. Käck, and G. Wendin, Phys. Rev. Lett. **88**, 046802 (2002).

- [16] R. J. Schoelkopf, P. Wahlgren, A. A. Kozhevnikov, P. Delsing, and D. E. Prober, *Science* **280**, 1238 (1998).
- [17] S. Hershfield, J. H. Davies, P. Hyldgaard, C. J. Stanton, and J. W. Wilkins, *Phys. Rev. B* **47**, 1967 (1993).
- [18] A. N. Korotkov, *Phys. Rev. B* **49**, 10381 (1994).
- [19] A. N. Korotkov, *Europhys. Lett.* **43**, 343 (1998).
- [20] A. M. van den Brink, *Europhys. Lett.* **58**, 562 (2002).
- [21] E. V. Sukhorukov, G. Burkard, and D. Loss, *Phys. Rev. B* **63**, 125315 (2001).
- [22] D. V. Averin and Y. V. Nazarov, in [55], chap. 6, p. 217.
- [23] D. C. Langreth, in *Linear and Nonlinear Transport in Solids*, edited by J. T. Devreese and V. E. van Doren (Plenum Press, New York, 1976), vol. 17 of *NATO ASI Series B: Physics*.
- [24] J. Rammer and H. Smith, *Rev. Mod. Phys.* **58**, 323 (1986).
- [25] K.-C. Chou, Z.-B. Su, B.-L. Hao, and L. Yu, *Phys. Rep.* **118**, 1 (1985).
- [26] J. König, J. Schmid, H. Schoeller, and G. Schön, *Phys. Rev. B* **54**, 16820 (1996).
- [27] Y. Isawa and H. Horii, *J. Phys. Soc. Jpn.* **69**, 655 (2000).
- [28] H. J. Spencer and S. Doniach, *Phys. Rev. Lett.* **18**, 23 (1967).
- [29] A. Kamenev and A. Andreev, *Phys. Rev. B* **60**, 2218 (1999).
- [30] D. B. Gutman and Y. Gefen, *Phys. Rev. B* **64**, 205317 (2001).
- [31] We adopt the time-path C used in Ref. [56] rather than the Keldysh contour $C_+ + C_-$ in Ref. [25], because the path C makes the formulation compact in the case where the initial state is in equilibrium.
- [32] In Ref. [25], the normalization condition of the generating functional is $Z|_{J=0} = 1$, viz. Z is normalized by Z_0 in advance.
- [33] D. C. Mattis, *The Theory of Magnetism*, vol. 17 of *Springer Series in Solid-State Sciences* (Springer-Verlag, Berlin Heidelberg New York, 1988), 2nd ed., p. 90.
- [34] V. S. Babichenko and A. N. Kozlov, *Solid State Commun.* **59**, 39 (1986).
- [35] The method to perform the path integral *directly* on C is demonstrated in an appendix of Refs. [36, 57]. A solution of differential equations defined on C is shown in an appendix of Ref. [36].
- [36] Y. Utsumi, H. Imamura, M. Hayashi, and H. Ebisawa, *Phys. Rev. B* **66**, 024513 (2002).
- [37] A. M. Zagoskin, *Quantum Theory of Many-Body Systems* (Springer-Verlag, New York, 1998).
- [38] Our treatment of the finite transport voltage is equivalent to the widely used one [58–63], where the voltage difference between two leads is included in the initial distribution function. Two treatments are related each other by a gauge transformation.
- [39] There are two differences between our definition and that in Ref. [30]. First, we use the generating functional for connected Green function W rather than Z , because we are interested in the correlation function of the current (or charge) *fluctuation* operator. Second, we propose the modified expression for the noise: Besides the standard definition, the first term of Eq. (29) or Eq. (30), we introduce the additional second term. It circumvents the uncertainty related to the order of operators (Appendix A).
- [40] S. Hershfield, J. H. Davies, and J. W. Wilkins, *Phys. Rev. B* **46**, 7046 (1992).
- [41] S. Hershfield, *Phys. Rev. B* **46**, 7061 (1992).
- [42] Our notations, $\alpha_r^K(\varepsilon)$ and $G_c^C(\varepsilon)$, correspond to $-2i\pi\alpha_r(\varepsilon)$ and $-2i\pi A(\varepsilon)$ in Ref. [6], respectively.
- [43] Y. Utsumi, H. Imamura, M. Hayashi, and H. Ebisawa, *Physica C* **367**, 237 (2002).
- [44] G. B. Lesovik, *JETP Lett.* **49**, 592 (1989).
- [45] Equation (42) in Ref. [18] is the corresponding result (for $T \ll E_C$). We adopt different notations and definitions; $S_{QQ}(0)$ corresponds to $S_{\varphi\varphi}(0) (2/C^2)$. $\Gamma_{L(R)I}$ and $\Gamma_{IL(R)}$ correspond to $\Gamma_{1(2)}^+$ and $\Gamma_{1(2)}^-$, respectively.
- [46] We confirmed that following numerical calculations achieve the spectral sum rule for c -field GF, $\int d\varepsilon G_c^C = -2i\pi$, up to 0.005%.
- [47] A. Shimizu and M. Ueda, *Phys. Rev. Lett.* **69**, 1403 (1992).
- [48] M. Ueda and A. Shimizu, *J. Phys. Soc. Jpn.* **62**, 2994 (1993).
- [49] V. A. Khlus, *Sov. Phys. JETP* **66**, 1243 (1987).
- [50] Y. Utsumi, H. Imamura, M. Hayashi, and H. Ebisawa, to appear in proceedings of *The International Symposium on Mesoscopic Superconductivity and Spintronics (MS+S2002)* (cond-mat/0205114).
- [51] Y. Utsumi, H. Imamura, M. Hayashi, and H. Ebisawa, to appear in proceedings of *The 23rd International Conference of Low Temperature Physics (August 20-27, 2002, Hiroshima)* (cond-mat/0211036).
- [52] W. Belzig and Y. V. Nazarov, *Phys. Rev. Lett.* **87**, 067006 (2001).
- [53] D. A. Bagrets and Y. V. Nazarov, cond-mat/0207624 (unpublished).
- [54] We can confirm the term $\text{Tr}[\tau^1 \tilde{\Sigma}_r \tau^1 \tilde{g}_c] = \Sigma_r^A g_c^A + \Sigma_r^R g_c^R$ is 0 from the analytic properties of the step function $\int d\varepsilon' 1/((\varepsilon' + \varepsilon + i\eta)(\varepsilon + i\eta)) = 0$, viz. $\theta(t)\theta(-t) = 0$. The standard definition for noise, the first term of Eq. (29) or Eq. (30), includes such terms, and thus one must remove them carefully. Our definition does not include such terms, which simplifies practical calculations for the second moment.
- [55] H. Grabert and M. H. Devoret, eds., *Single Charge Tunneling*, vol. 294 of *NATO ASI Series B* (Plenum Press, New York and London, 1992).
- [56] M. N. Kiselev and R. Oppermann, *Phys. Rev. Lett.* **85**, 5631 (2000).
- [57] K. Okumura and Y. Tanimura, *Phys. Rev. E* **53**, 214 (1996).
- [58] C. Caroli, R. Combescot, P. Nozieres, and D. Saint-James, *J. Phys.* **C4** p. 916 (1971).
- [59] C. Caroli, R. Combescot, D. Lederer, P. Nozieres, and D. Saint-James, *J. Phys.* **C4** p. 2598 (1971).
- [60] R. Combescot, *J. Phys.* **C4** p. 2611 (1971).
- [61] C. Caroli, R. Combescot, P. Nozieres, and D. Saint-James, *J. Phys.* **C5** p. 21 (1972).
- [62] Y. Isawa and M. Kanechika, *J. Phys. Soc. Jpn.* **60**, 4013 (1991).
- [63] Y. Meir and N. S. Wingreen, *Phys. Rev. Lett.* **68**, 2512 (1992).